Development 122, 3969-3979 (1996)
Printed in Great Britain © The Company of Biologists Limited 1996
DEV6253

Joint patterning defects caused by single and double mutations in members of the bone morphogenetic protein (BMP) family

Elaine E. Storm and David M. Kingsley*

Department of Developmental Biology, Beckman Center B300, Stanford University School of Medicine, Stanford, CA 94305-5427, USA

*Author for correspondence (e-mail: hf.dmk@forsythe.stanford.edu)

SUMMARY

The mouse *brachypodism* locus encodes a bone morphogenetic protein (BMP)-like molecule called growth/differentiation factor 5 (GDF5). Here we show that *Gdf5* transcripts are expressed in a striking pattern of transverse stripes within many skeletal precursors in the developing limb. The number, location and time of appearance of these stripes corresponds to the sites where joints will later form between skeletal elements. Null mutations in *Gdf5* disrupt the formation of more than 30% of the synovial joints in the limb, leading to complete or partial fusions between particular skeletal elements, and changes in the patterns of repeating structures in the digits, wrists and ankles. Mice carrying null mutations in both *Gdf5* and another BMP family member, *Bmp5*, show additional abnormalities not observed in either of the single mutants. These defects include disruption of the sternebrae within the sternum and abnormal formation of the fibrocartilaginous joints between the sternebrae and ribs. Previous studies have shown that members of the BMP family are required for normal development of cartilage and bone. The current studies suggest that particular BMP family members may also play an essential role in the segmentation process that cleaves skeletal precursors into separate elements. This process helps determine the number of elements in repeating series in both limbs and sternum, and is required for normal generation of the functional articulations between many adjacent structures in the vertebrate skeleton.

Key words: growth/differentiation factor 5, bone morphogenetic protein, mouse mutation, skeletal patterning, joint

INTRODUCTION

The skeletal elements of the vertebrate limb are derived during embryonic development from mesenchymal cells, which condense and initiate a differentiation program that results in cartilage and bone. The diverse shapes and patterns of skeletal elements arise from several fundamental morphogenetic behaviors of the limb mesenchyme (Shubin and Alberch, 1986; Oster et al., 1988). These behaviors include the initial de novo condensation of cells into the rough outlines of the future skeletal elements, the growth and branching of some of the condensations to produce Y-shaped bifurcations, and the segmentation of condensations into individual elements. For example, the humerus, radius and ulna of the forelimb arise initially from a single condensation that grows, branches and segments to produce the precursors of the three separate bones. Variations in the temporal and spatial patterns of condensation, branching and segmentation underlie much of the evolutionary modifications of limb structures that are seen in different vertebrate species (Shubin and Alberch, 1986; Oster et al., 1988).

Despite the importance of mesenchymal condensations in skeletal patterning, relatively little is known about the factors that control their formation, branching and segmentation (Hall and Miyake, 1992). Recent studies, however, suggest that bone morphogenetic proteins (BMPs) may play a crucial rule in inducing the formation of particular skeletal condensations. BMPs were originally purified from adult bones based on their remarkable ability to trigger the entire sequence of condensation, cartilage differentiation and bone formation when implanted at ectopic sites in animals (Urist, 1965; Reddi and Huggins, 1972). Biochemical purification, cloning studies and homology screens have shown that the vertebrate genome contains a large number of related BMPs, most of which belong to the transforming growth factor beta (TGF-β) family of secreted signalling molecules (Rosen and Thies, 1992; Kingsley, 1994a,b for review). Particular members of the BMP family are expressed at times and places consistent with a role in inducing the formation of early skeletal condensations (Lyons et al., 1989; King et al., 1994). Null mutations in the *Bmp5* gene have also been shown to reduce or eliminate particular skeletal condensations during normal mouse development, confirming an essential role for this signal in formation of particular anatomical features in the skeleton (Kingsley et al., 1992, 1994b; King et al., 1994).

We recently reported that the mouse *brachypodism* locus encodes a new member of the BMP family called growth differentiation factor 5 (GDF5) (Storm et al., 1994). Mutations at this locus have been studied for forty years because of their interesting effects on the pattern of repeating elements in the

vertebrate limb (Landauer, 1952; Grüneberg and Lee, 1973; Elmer and Selleck, 1975; Hinchliffe and Johnson, 1980). *Brachypodism* mutations reduce the length of several long bones of the limb, and cause the first two bones in most digits to be replaced by a single element. Molecular studies have shown that these limb-patterning defects are due to frame-shift mutations in the *Gdf5* gene (Storm et al., 1994). Although these mutations should completely inactivate *Gdf5*, *brachypodism* mice are viable and fertile, and show little defects in skeletal structures outside the limbs.

In order to gain insight into how *Gdf5* participates in skeletal patterning, we have undertaken a detailed analysis of RNA expression during limb development and have generated double mutants that lack two different BMPs: *Gdf5* and *Bmp5*. These combined studies suggest that BMP family members may play important roles not only in generating early skeletal condensations, but also in controlling the segmentation events that generate the joints between skeletal structures.

MATERIALS AND METHODS

Mice

The bp^J and bp^{3J} alleles occurred spontaneously on the inbred A/J and BALB/cJ strains, respectively, and were maintained on the corresponding isogenic backgrounds. The se^{2OZb} mutation is a null allele at the *Bmp5* locus and is maintained on an outbred background (Kingsley et al., 1992). Double mutants were generated by crossing bp^J or bp^{3J} homozygotes to se^{2OZb} homozygotes, intercrossing the F_1 progeny and collecting short-eared animals with short feet and limbs. Double mutants were maintained by intercrossing.

In situ hybridization

The mouse *Gdf5* probe was generated from a 267 bp PCR product in the 3′ untranslated region (bases 1837-2103, Storm et al., 1994) cloned into pCR™II (Invitrogen). The mouse *Bmp5* probe was generated from a 1.03 kb PCR product of the pro-region of the cDNA (bases 671-1702, King et al., 1994) cloned into pCR™II (Invitrogen). Digoxigenin (DIG) cRNA probes were prepared using the Genius™ 4 kit (Boehringer Mannheim).

Timed matings were performed and embryonic day 0.5 was designated as noon on the day a vaginal plug was observed. Embryos were dissected in cold PBS and frozen quickly on dry ice in OCT compound (Miles). Frozen tissue was stored at −80°C until sectioned at 12 μm on Vectabond™ (Vector)-treated slides at −20°C. In situ hybridization was carried out using a modification of previous protocols (Schaeren-Wiemers and Gerfin-Moser, 1993). Sections were dried at room temperature for 20-30 minutes, fixed in 4% paraformaldehyde/PBS for 10 minutes, washed three times for 3 minutes in PBS, acetylated 10 minutes (1.1% triethanolamine, 0.25% acetic anhydride), washed three times for 5 minutes in PBS, prehybridized in 200 μl hybridization buffer [50% formamide (GibcoBRL), 5× SSC, 5× Denhardt's, 250 μg/ml baker's yeast RNA (Sigma), 500 μg/ml sonicated salmon sperm (Sigma)] for 3-6 hours at room temperature in a 50% formamide/5× SSC humidified chamber and hybridized with DIG-cRNA (200 ng/ml) in hybridization buffer for 16-20 hours at 60°C under Parafilm in a 50% formamide/5× SSC humidified chamber.

Following hybridization, sections were rinsed in 5× SSC at 60°C, washed in 0.2× SSC at 60°C for 1 hour, rinsed in B1 (0.1 M maleic acid, 0.15 M sodium chloride, pH 7.5) for 5 minutes, blocked in 1% blocking reagent (Boehringer Mannheim)/B1 for 1 hour, incubated with anti-digoxigenin antibodies (Boehringer Mannheim) at a dilution of 1:5,000 in B1 for 1 hour, washed in B1 two times for 15 minutes, rinsed in B3 (100 mM Tris-HCl, 100 mM sodium chloride, 5 mM magnesium chloride, pH 9.5) 5 minutes and developed 24-48 hours in B4 (0.24 mg/ml levamisole, 3.38 mg/ml 4-nitroblue tetrazolium chloride and 1.75 mg/ml 5-bromo-4-chloro-3-indolyl phosphate (Sigma) in B3). The color reaction was stopped in 100 mM Tris-HCl, 1 mM EDTA, pH 8.0. Some slides were counterstained in 1% aqueous Eosin Y (Sigma) for 30 seconds and rinsed in running tap water for 5 minutes. Slides were mounted with Aqua-mount (Lerner-Laboratories).

Histological and skeletal analysis

Embryos were dissected in cold PBS, fixed overnight in 4% paraformaldehyde/PBS, dehydrated through an ethanol series in 0.85% saline, clarified in toluene and xylene, and embedded in paraffin (Polysciences). 8 μm sections were stained with Harris Hematoxylin and Eosin Y (Sigma).

Skeletal preparations were made from 27- to 29-day-old mice (Lufkin et al., 1992). Bone lengths were measured from female mice using a 0.01 mm resolution sliding caliper (Table 2). All other skeletal data is based on pooled results from males and females.

RESULTS

Gdf5 expression during limb development

The skeletal elements of the limb are formed in a proximal-to-distal sequence beginning with the formation of the condensation for the humerus at day 10.5 dpc (Dalgleish, 1964; Wanek et al., 1989). This condensation later branches distally to form condensations for the ulna and radius (11.5 dpc). Condensations for the digits begin as continuous structures (digital rays) that lengthen distally during limb bud outgrowth. These rays are cleaved by sequential transverse segmentation events to generate the metacarpals and the phalanges of the forefeet (days 13.5-15.5 dpc).

Gdf5 expression is first detected in the developing forelimb on day 11.5 dpc (stage 5 in the Wanek et al., 1989 system). At this stage, expression is seen primarily in a proximal and distal region that correspond to the site where the shoulder and elbow will later form (Fig. 1A,B). In more advanced 11.5 day embryos (stages 6 and 7) expression extends into the developing handplate to include lower level interdigital expression as well as expression in the palmar arch (data not shown).

One day later (12.5 dpc, stage 8) *Gdf5* continues to be expressed in the developing shoulder (Fig. 1D,E) and elbow (data not shown). Additionally, a new site of strong expression appears within the developing digital ray. This site of expression coincides with the region of the future joint between the metacarpals and the proximal phalanges. Expression extends proximally along the outer perimeter of the metacarpal. Lower level expression is also detected interdigitally, in the region of the developing carpals, as well as distally within the digital ray, (data not shown).

At 13.5 dpc (stages 9 and 10), *Gdf5* is clearly expressed in the developing shoulder and elbow joints (Fig. 1G), and in the presumptive joint region between the metacarpals and the proximal phalanges (Fig. 1H and data not shown). In addition, *Gdf5* is now expressed between the developing rows of carpals and in an additional stripe across the digital rays (Fig. 1H). These sites of expression correspond to the developing joints of the wrist and the first interphalangeal joint, respectively. There is also continued lower level expression around the

metacarpals and in the interdigital mesenchyme (data not shown).

By 14.5 dpc (stage 11), all of the skeletal elements of the forelimb are present and are undergoing chondrogenesis. At this stage, an additional stripe appears in the digital ray separating the developing medial phalanges from the distal phalanges (Fig. 1I). In more proximal regions of the limb, *Gdf5* expression is clearly seen in the joint region and developing articular surfaces. After 15.5 dpc, *Gdf5* expression decreases (data not shown). Due to an increase in background with this technique at this stage, however, it is possible that expression continues below the level of detection.

Similar expression of *Gdf5* is observed in the analogous joints and skeletal elements in the hindlimb (data not shown). As in the forelimb, expression occurs in the same proximo-distal sequence as the normal joint formation (Dalgleish, 1964; Mitrovic, 1978; Wanek et al., 1989), and precedes any morphological sign of joint formation.

Joint defects in *brachypodism* mutant mice

Previous studies of *brachypodism* mice have shown that the number of phalanges is reduced from three to two in digits II-V of all four feet.

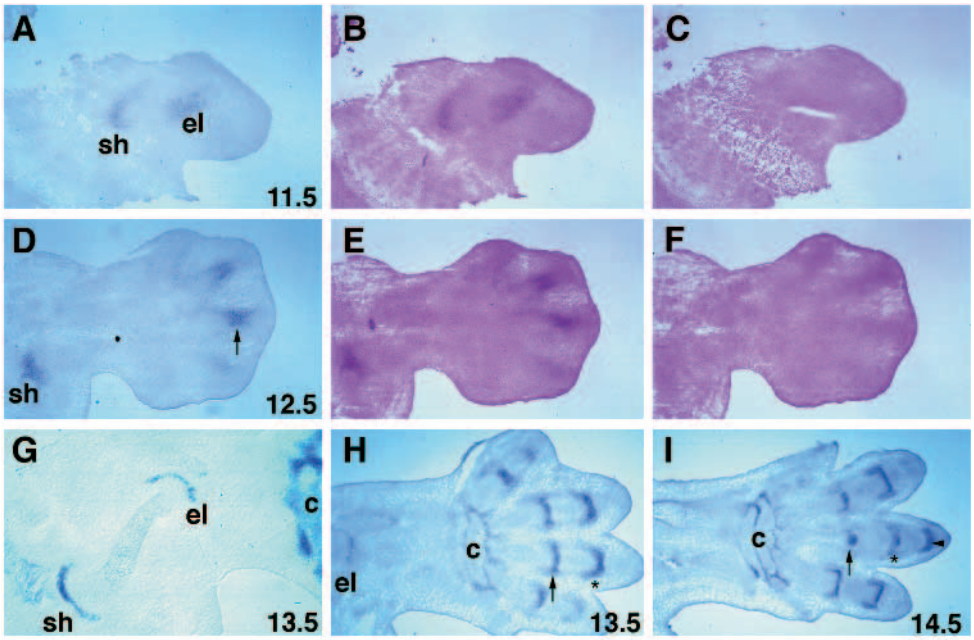

Fig. 1. RNA expression of *Gdf5* during limb development is primarily restricted to regions of joint formation. Forelimb sections from 11.5-14.5 dpc embryos were hybridized with antisense (A,B,D,E,G-I) and sense (C,F) probes from the *Gdf5* 3-prime untranslated region. Proximal is to the left, anterior is down. (A) 11.5 dpc forelimb showing expression in the developing shoulder (sh) and elbow (el) joints. (D) 12.5 dpc forelimb. *Gdf5* continues to be expressed in the shoulder (sh) and elbow (out of the plane of section). Strong *Gdf5* expression appears in the digital ray, corresponding to the site of the future metacarpo-phalangeal joint (arrow). Expression is also seen along the perimeter of the developing metacarpal and in the interdigital mesenchyme. (B,E) Sections adjacent to A and D, counterstained with aqueous Eosin. (C,F) Section adjacent to B and E, hybridized with the sense probe and counterstained with Eosin. *Gdf5* expression precedes any morphological indication of joint development in the shoulder, elbow, and metacarpo-phalangeal joint. (G,H) 13.5 dpc forelimbs. *Gdf5* expression in the shoulder (sh) and elbow (el) is clearly localized to the joint region (G). Additional stripes of expression are now seen between the developing rows of carpals (c, H), and at the site where the first interphalangeal joint will develop in the digital rays (*, H). (I) 14.5 dpc forelimb. A third stripe is now evident in the digital ray (arrowhead), corresponding to the site where the second interphalangeal joint will form. Continued expression is also seen in the elbow (not shown), carpals (c), and more proximal stripes (arrow, *) in the digital rays.

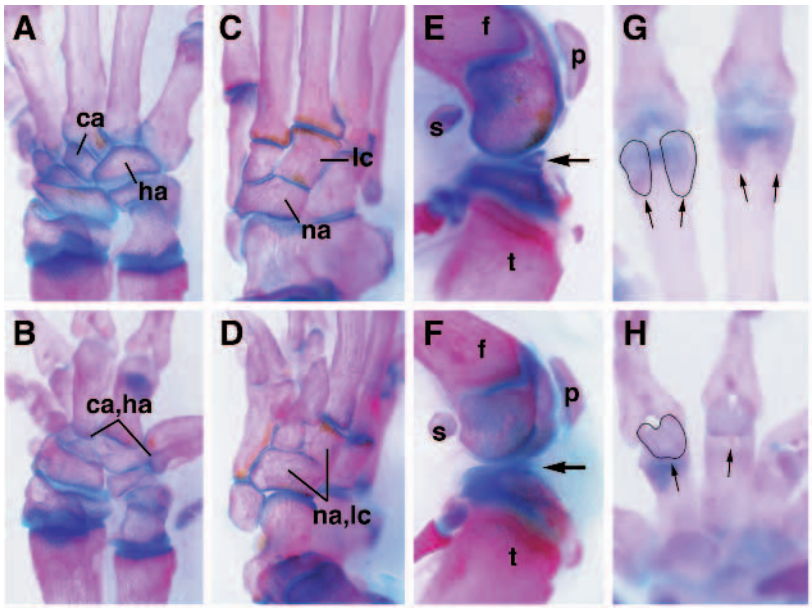

Fig. 2. Examples of joint defects in bp^{3J}/bp^{3J} mice. Adult, age-matched skeletons from $bp^{3J}/+$ (A,C,E,G) and bp^{3J}/bp^{3J} (B, D, F, H) animals were stained with alizarin red (mineralized elements) and Alcian blue (non-mineralized cartilage). (A,B) Dorsal view of right forefeet showing wild-type pattern of carpal development (A) and fusion of capitate (ca) and hamate (ha) in bp^{3J}/bp^{3J} homozygotes (B). (C,D) Dorsal view of right hindfeet showing wild-type pattern of tarsal development (C) and partial fusion of navicular (na) and lateral cuneiform (lc) in bp^{3J}/bp^{3J} homozygotes (D). (E,F) Lateral view of right knees from $bp^{3J}/+$ (E) and bp^{3J}/bp^{3J} (F) animals. f, femur; t, tibia; p, patella; s, lateral sesamoid; arrow indicates the meniscus. Note that the meniscus is not mineralized in bp^{3J}/bp^{3J} homozygotes (F). (G,H) Ventral view of digits III and IV in right forefoot showing the wild-type pattern of sesamoids at the base of the proximal phalanges (G), and fusions of the sesamoids in bp^{3J}/bp^{3J} homozygote (H). The sesamoids of digits IV have been outlined for emphasis.

The altered number of phalanges arises from a failure to cleave the early digital ray between the proximal and medial phalanges during embryogenesis (Milaire, 1965; Grüneberg and Lee, 1973). *Gdf5* is normally expressed in a stripe at this cleavage site, suggesting that *Gdf5* may be directly required for formation of this joint. Interestingly, *Gdf5* is also expressed in most of the other developing joints in the limb. To determine whether this expression corresponds with other *brachypodism* phenotypes, we compared adult skeletal preparations of bp^{3J}/bp^{3J} and $bp^{3J}/+$ mice. The bp^{3J} mutation occurred on an inbred genetic background providing the first opportunity to compare the effects of *Gdf5* mutations in animals that differ only at the *brachypodism* locus.

In the adult skeletons of *brachypodism* mice, we observed several highly penetrant phenotypes in the knee, the forefeet and the hindfeet, suggesting that *Gdf5* is required for the normal development of several additional joints and skeletal structures in the limb (Table 1 and Fig. 2). The phenotypes in bp^{3J} homozygotes included many partial or complete fusions between bones in both the wrist and ankle (Fig. 2A-D). Additional fusions were seen in the developing digits, including fusions between the proximal and medial phalanges of digits II-V as previously described (Landauer, 1952; Grüneberg and Lee, 1973), between metacarpal V and the distal element in the forefoot, and between the small sesamoid bones at the metacarpo-phalangeal joints of digits III and IV in the forefoot (Fig. 2G,H). In addition, several skeletal structures were either absent or reduced in size, including one of the two metacarpo-phalangeal sesamoids of digit II, the medial sesamoids in the knee and the metatarsal growth plates of digits II and V (Table 1). Finally, the knee joint showed obvious changes in structure, including medial displacement of the patella and failure to mineralize the menisci (Fig. 2E,F).

Table 1. Summary of phenotypes in bp^{3J}/bp^{3J} mice

	$bp^{3J}/+$	bp^{3J}/bp^{3J}
Partial/complete fusion of elements		
Forefoot		
carpals*	1/14	20/24
capitate/hamate	0	12
centrale/capitate/hamate	0	6
other	1†	2‡
metacarpal/proximal phalanx, digit V	0/14	19/24
proximal/medial phalanges, digits II-V	0/14	24/24
metacarpo-phalangeal sesamoids, digits III and IV	0/14	24/24
Hindfoot		
tarsals (navicular/lateral cuneiform)	0/14	16/24
proximal/medial phalanges, digits II-V	0/14	24/24
Other joint abnormalities		
Knee		
medial displacement of the patella	0/14	22/24
failure to mineralize the menisci	0/14	24/24
Absence/reduction of structures		
Forefoot		
1 of 2 metacarpo-phalangeal sesamoids, digit II	0/14	22/24
Hindfoot		
metatarsal growth plates, digits II and V	0/14	24/24
Knee		
medial sesamoid	0/14	22/24

Ratios indicate the number of affected elements/number of elements examined.
*Total number of wrists with fused carpals.
†trapezoid/centrale fused.
‡trapezoid/centrale and capitate/hamate fused.

Generation of *short ear; brachypodism* double mutants

Several joints in the limb strongly express *Gdf5* but do not show obvious phenotypes in mutant mice, including the shoulder, the elbow and the second interphalangeal joints. This raises the possibility that related molecules may be able to compensate for the loss of *Gdf5* at other sites in the embryo. To test this possibility, we generated double mutant mice that lack functional copies of both *Gdf5* and *Bmp5*, the only other BMP gene for which viable mutations were available when we began these studies. Previous studies have shown that *Bmp5* is expressed in early skeletal condensations and the perichon-

Table 2. Limb effects in *short ear; brachypodism* double mutant animals

	se/+; bp^{J}*/+*	*se/se; bp*^{J}*/+*	*se/+; bp*^{J}*/bp*^{J}	*se/se; bp*^{J}*/bp*^{J}
Mean length of long bones (mm ± s.d.)*	(38)	(38)	(64)	(30)
Forelimb				
humerus	9.8±0.4	9.3±0.6	8.6±0.6	8.4±0.5
ulna	11.2±0.4	10.8±0.6†	10.5±0.6	10.1±0.5
radius	8.9±0.4	8.6±0.6	8.4±0.5‡	8.2±0.5
Hindlimb				
femur	11.8±0.6	11.2±0.8	8.8±0.7	8.8±0.8
tibia	13.8±0.6	13.2±0.9	11.4±0.8	10.8±0.6
fibula	12.7±0.5	12.2±0.8	5.4±1.9‡	1.9±1.4
Knee Sesamoids§	(82)	(86)	(114)	(82)
Medial				
reduced	7.3%	29%	22%	0%
absent	1.2%	66%	41%	99%
Lateral				
reduced	0%	21%	9.6%	38%
absent	0%	4.6%	0%	39%

*Long bones from age-matched females were measured using sliding calipers. Number of elements measured are indicated in parentheses unless otherwise noted.
†Mean calculated from 36 ulnae.
‡Mean claculated from 63 elements.
§Percentages refer to the number of sesamoids either reduced or absent. The total number examined is indicated in parentheses.

drium surrounding particular skeletal elements (King et al., 1994, 1996). Null mutations in *Bmp5* reduce the size, shape and number of many different cartilage and bone elements, including the external ear (Green, 1968; Kingsley et al., 1992, 1994). To generate double mutant animals, se^{2OZb} homozygous mice (carrying a null mutation in *Bmp5*) were first crossed to bp^J homozygotes (carrying a null mutation in *Gdf5*). The F_1 progeny animals ($se^{2OZb}/+$; $bp^J/+$) were then intercrossed to generate 9 different theoretical combinations of alleles at the *se* and *bp* loci (animals wild type, heterozygous, or homozygous for mutations at each of two different genes). All of the F_2 progeny fell into the four phenotypic classes expected for independent segregation of two different recessive mutations controlling ear and limb length: 119 animals with normal ear and limb length (*?/+; ?/+*), 43 animals with long ears and short limbs (*?/+;* bp^J/bp^J), 38 animals with short ears and long limbs (se^{2OZb}/se^{2OZb}; *?/+*), and 11 double mutant progeny with short ears and short limbs (se^{2OZb}/se^{2OZb}; bp^J/bp^J). Each phenotypic class occurred in the expected phenotypic ratio of 9:3:3:1 (Chi-square test for deviation=0.558, $P > 0.9$). The double mutant animals were fertile and produced 100% short-eared, short-limbed progeny when intercrossed, confirming that they were homozygous for mutations at both the *se* and *bp* loci.

For more detailed analysis of skeletal phenotypes, additional crosses were set up between $se^{2OZb}/+$; $bp^J/+$ compound heterozygotes and the viable se^{2OZb}/se^{2OZb}; bp^J/bp^J double mutants. This configuration generates four classes of progeny that are homozygous for either the *brachypodism* mutation ($se^{2OZb}/+$; bp^J/bp^J), the *short ear* mutation (se^{2OZb}/se^{2OZb}; $bp^J/+$), both mutations (se^{2OZb}/se^{2OZb}; bp^J/bp^J), or neither mutation ($se^{2OZb}/+$; $bp^J/+$). The genotype of each animal can be determined unambiguously by simple inspection of ear and limb length, and all four classes of progeny occur in sufficient numbers to allow detailed comparisons of skeletal phenotypes associated with loss of one or both genes.

Limb phenotypes in single and double mutant animals

Previous studies have shown that homozygosity for the *brachypodism* mutation reduces the length of various long

Table 3. Summary of sternum phenotypes in *short ear; brachypodism* double mutant animals

	se/+; bp^J/+	*se/se; bp^J/+*	*se/+; bp^J/bp^J*	*se/se; bp^J/bp^J*
A. Missing sternebrae				
Total animals affected	0/42	0/43	1/58	41/41
manubrium	0	0	0	0
sternebra 1	0	0	0	14
sternebra 2	0	0	1	41
sternebra 3	0	0	0	4
sternebra 4	0	0	0	0
B. Affected sternal joints*				
Total animals affected	6/42	26/43	55/58	41/41
RS1	0	0	0	0
RS2	4	14	41	31
RS3	0	0	50	41
RS4	0	1	3	41
RS5	2	14	4	29
(i) Sternebrae segmentation†				
Total animals affected	4/42	20/43	8/58	33/41
RS2 r+	2	1	0	4
r–	0	7	4	9
RS5 r+	2	13	2	27
r–	0	0	2	0
(ii) Rib/sternal segmentation‡				
Total animals affected	1/42	0/43	0/58	40/41
RS1	0	0	0	0
RS2	1	0	0	13§
RS3	0	0	0	39¶
RS4	0	0	0	26‖
RS5	0	0	0	2**
(iii) Ectopic mineralization††				
Total animals affected	1/42	7/43	55/58	39/41
RS2	1/42	6/25	37/54	12/25
RS3	0/42	0/43	50/55	23/23
RS4	0/42	1/43	3/55	38/38
RS5	0/42	1/30	0/54	2/13

*Total animals with at least one sternocostal joint defect. RS1-RS5 denotes junctions where rib pairs 1-5 meet the sternum, respectively.

†Total number of animals whose sternocostal joint abnormalities include a complete failure of the sternebrae to segment. RS2, fusion of the manubrium and sternebra 1. RS5, fusion of sternebrae 3 and 4. r+, ribs were present at the sternum. r-, ribs did not reach the sternum

‡Total number of animals whose sternocostal joint abnormalities include partial or complete fusion of either rib with the sternum.

§3/23 (13%) animals had RS2 rib fusions between two normal sternebrae, 10/18 (56%) had RS2 rib fusions adjacent to a single missing sternebra.

¶21/23 (91%) animals had RS3 rib fusions adjacent to a single missing sternebra, 18/18 (100%) had rib fusions between two missing sternebrae.

‖23/37 (62%) animals had RS4 rib fusions adjacent to a single missing sternebra, 3/4 (75%) had rib fusions between two missing sternebrae

**1/37 (2.7%) animals had RS5 rib fusions between two normal sternebrae, 1/4 (25%) had rib fusions adjacent to a single missing sternebra

††Total number of animals whose sternocostal joint abnormalities include ectopic mineralization in the fibrocartilage of the joint. Does not include animals with complete fusion of sternebrae or animals where rib fusions ocurr between two missing sternebrae.

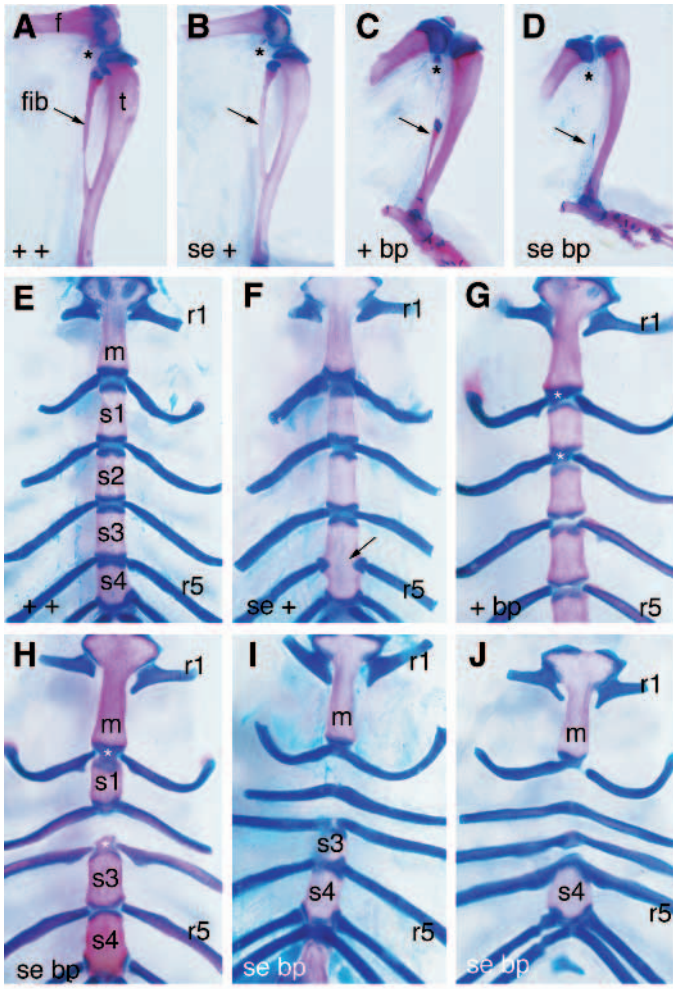

Fig. 3. Loss of both *Gdf5* and *Bmp5* results in synergistic phenotypes in the hindlimbs and the sternum. Alizarin-red/Alcian-blue-stained skeletons were prepared from animals from the *short ear; brachypodism* double mutant cross. (A) Right hind limb from a *se/+; bp/+* animal showing normal femur (f), tibia (t), fibula (fib) and lateral sesamoid of knee (*). (B) The hindlimbs from *se/se; bp/+* animals look similar. (C) Hindlimb from a *se/+; bp/bp* animal. The limbs are noticeably shorter and the fibula is disproportionately reduced (arrow). (D) The hindlimbs from *se/se; bp/bp* double mutant animals show greater reductions in length. Both the lateral sesamoid (*) and the fibula are severely affected by the absence of *Gdf5* and *Bmp5*, suggesting a synergistic interaction in the development of these elements. (E) *se/+; bp/+* sternum showing the wild-type pattern of elements. m, manubrium; s1-s4, sternebrae 1-4; r1, r5, rib pairs 1 and 5. Note that all rib pairs except the first form compound joints with the adjacent sternebrae. (F) *se/se; bp/+* sternum. Fusion of sternebrae 3 and 4 (arrow) is observed in 30% of *se/se; bp/+* animals in our cross and has previously been observed in other *short ear* alleles. (G) *se/+; bp/bp* sternum. The manubrium, ribs and sternebrae are grossly normal. Note the ectopic mineralization in the sterno-costal joint where rib pairs 2 and 3 articulate (*). (H-J) Three different examples of sternums from *se/se; bp/bp* double mutant mice. (H) Sternebrae 2 is missing, rib pair 3 is partially fused with sternebra 1, and ectopic mineralization is present (*) where rib pairs 2 and 4 meet the sternum. (I,J) Additional sternebrae are missing and one or more rib pairs are fused across the midline or with adjacent sternebrae.

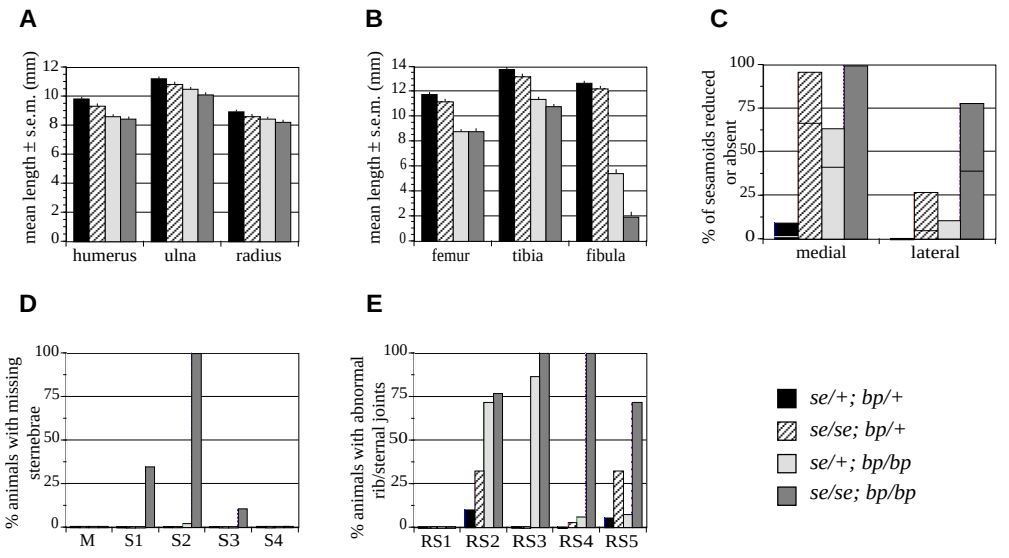

Fig. 4. Summary of the effects of single and double mutations on limb and sternum development. (A,B) Mean lengths of forelimb (A) and hindlimb (B) elements show additive length reductions by the *se* and *bp* mutations in most bones, but synergistic effects on reducing the length of the fibula. (C) The percentages of knee sesamoids that are lost or reduced in single and double mutants also reveal a synergistic effect of *Bmp5* and *Gdf5* mutations on development of the lateral sesamoid. Lines within bars represent the % of sesamoids that were completely absent in the different genotypes. (D) Percentage of animals with missing sternal elements. M, manubrium; S1-S4, sternebrae 1-4 respectively. With the exception of a single *se/+; bp/bp* animal with a missing sternebra 2, missing sternebrae were only observed in double mutants. This effect is strongest in the midportion of the sternum. (E) Percentage of animals with abnormal joints at the points where rib pairs 1-5 meet the sternum (RS1-RS5). Homozygosity for the *se* mutation affects a small percentage of rostral and caudal rib/sternal joints. Homozygosity for the *bp* mutation affects a large percentage of RS2 and RS3 joints. The *se/se; bp/bp* double mutants have defects in a higher percentage of joints throughout the sternum including RS4, a joint not affected by either of the single mutants.

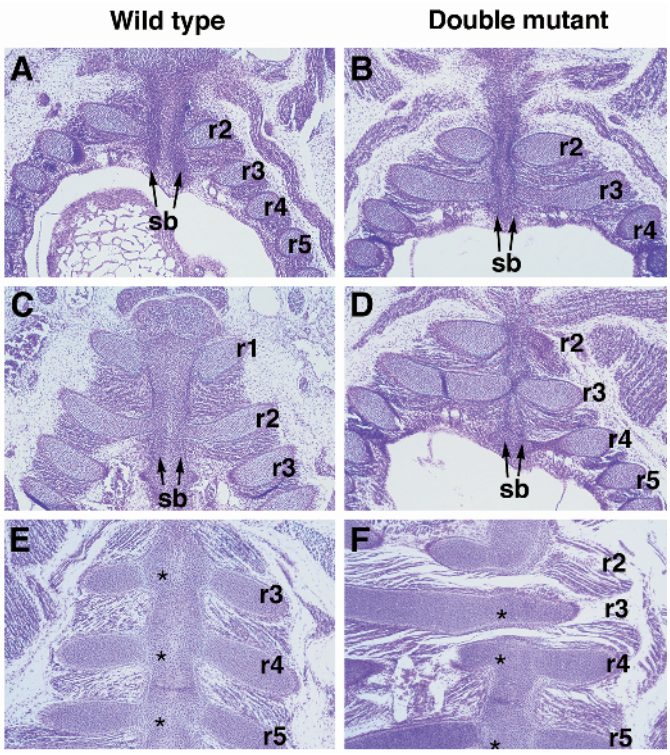

Fig. 5. The sternal bands are present but fail to differentiate and segment normally in double mutant mice. Sections stained with Hematoxylin and Eosin from wild-type and double mutant embryos at consecutive stages of sternum development. Rostral is to the top. (A) Wild-type embryo, 14.5 dpc. The sternal bands and ribs are beginning to meet at the ventral midline. sb, sternal bands; r2-5, rib pairs 2-5 respectively. (B) Double mutant embryo at stage similar to (A). The sternal bands are present and continuous at the ventral midline, as in wild type. (C) Wild-type embryo, 15.0 dpc. The sternal bands have increased in thickness and are beginning to fuse at the midline. (D) Double mutant embryo at stage similar to (C). The sternal bands in the affected region (rib pairs 3 and 4) are still visible, but have not increased in thickness. (E) Wild-type embryo, 16.5 dpc. Cellular differences at the rib/sternum junction (*) indicate the beginnings of segmentation of the sternebrae and ribs. (F) Double mutant embryo, 16.5 dpc. The sternal bands between rib pairs 2 and 3, and 3 and 4 have not developed into cartilage. Ribs have fused across the midline and muscle and connective tissue fill the adjoining spaces. At more rostral and caudal regions of the sternum, sternebrae and ribs are both present. Regional differences in cellular differentiation and matrix production are less apparent than in wild type (*).

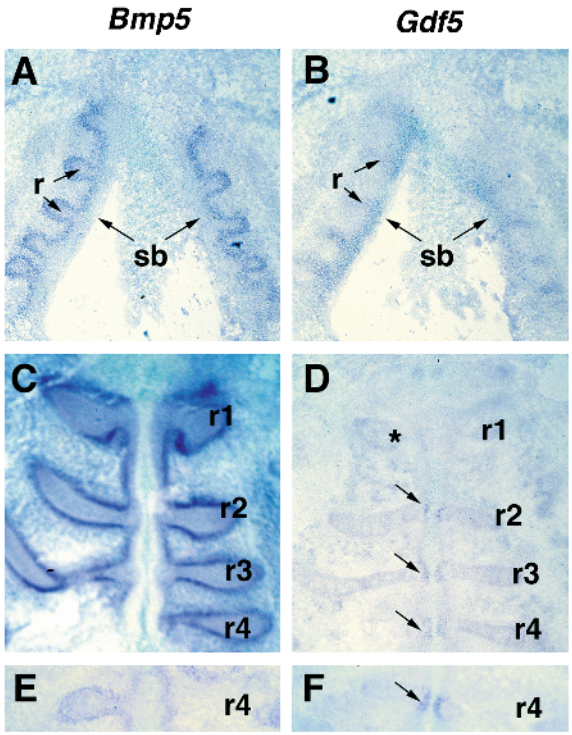

Fig. 6. *Bmp5* and *Gdf5* are expressed in non-overlapping patterns during sternum development. Adjacent frontal sections from wild-type mice at various stages of sternum development were hybridized with either *Bmp5* or *Gdf5* antisense RNA probes. (A,C,E) *Bmp5* is expressed in the perichondrium surrounding sternal bands (sb) and ribs both before and after the sternal bands reach the ventral midline (A, stage 2; C and E, stage 4, 14.5 dpc). (B) *Gdf5* is expressed in a complementary pattern within the sternal bands and ribs at early stages (stage 2, section adjacent to A). (D,F) At later stages, *Gdf5* is expressed in stripes where the ribs contact the sternum (see arrows, stage 4, sections adjacent to C and E). Note that *Gdf5* is not expressed where rib pair 1 (r1) touches the sternum (*). Sternum segmentation does not take place at this site in mice or most other mammals (Parker, 1867).

bones in the limb by 4 to 20% (Landauer, 1952; Grüneberg and Lee, 1973). The *short ear* mutation has smaller effects on the length of long bones, ranging from little effect to reductions of 7% or less (Green, 1968; Mikic et al., 1995, 1996). In our cross, homozygosity for either the *brachypodism* mutation or the *short ear* mutation also reduced the length of particular limb elements (see Table 2; Figs 3, 4). In animals homozygous for both mutations, the limb bones showed greater reductions in length (Fig. 3; Table 2). The reductions of most long bones (humerus, ulna, radius, femur and tibia) were consistent with the lengths expected from the combined effects of each of the individual mutations. The reduction in the length of the fibula, however, was much larger than expected, suggesting that loss of both *Bmp5* and *Gdf5* has a synergistic effect on development of this bone.

A similar synergistic interaction was observed in the development of the lateral sesamoid of the knee. Homozygosity for mutations in either *Bmp5* or *Gdf5* individually affected the presence and size of this sesamoid (Table 2; Figs 3, 4C). In double homozygotes, however, more sesamoids were affected (77%) and a larger proportion were completely absent. This phenotype is stronger than expected based on the phenotypes of each of the single mutants. Interestingly, the medial sesamoid did not show the same synergistic interaction in the double mutants (Table 2; Fig. 4C). The more severe phenotype observed in the *se/se; bp/bp* mice is consistent with the combined effect of each of the two mutations. These results suggest that *Bmp5* and *Gdf5* mutations have independent or additive affects on the development of many of the skeletal structures in the limbs (the length of most of the long bones, the development of the medial sesamoid) as well as synergistic affects on the development of particular elements (the fibula and the lateral sesamoid).

Sternum effects in single and double mutant animals

The most dramatic new phenotypes in the double mutant were observed in the sternum. The wild-type sternum is a segmented structure consisting of a manubrium at the most rostral end, four segments called sternebrae and a xiphoid process at the caudal end (Fig. 3E). In 41 out of 41 double mutants, the second sternebra was completely missing (Figs 3H,J, 4D; Table 3). A substantial number of double mutant animals were also missing the first sternebra (14/41), and a few were missing sternebrae 1, 2 and 3 (4/41). In all sternums examined the phenotype was restricted to the midregion of the sternum; neither the manubrium nor the 4th sternebra were severely affected (Fig. 4D). Although the *short ear* mutation affected the most caudal segment of the sternum (the xiphoid process), the more rostral segments were always present. Similarly, the *brachypodism* mutation did not affect the development of any of the segments of the sternum. The strong effect of the combined *short ear* and *brachypodism* mutations suggests that BMP5 and GDF5 have a synergistic effect on development of particular regions of the sternum.

In addition to the loss of sternebrae, *se/se; bp/bp* double mutant mice also showed striking changes in the formation of the joints at the sterno-costal junctions (Figs 3, 4; Table 3). In wild-type mice, seven pairs of ribs articulate with the sternum. The first pair of ribs articulates at the rostral end of the manubrium. Each of the following four pairs of ribs articulate between adjacent sternebral segments, forming the sterno-costal junctions (Fig. 3E). These junctions are the site of compound fibrocartilaginous joints between the two adjacent sternebrae and the articulating rib pair (Chen, 1952a). The 6th and 7th pairs of ribs articulate between the fourth sternebra and the xiphoid process. Homozygosity for the *se* mutation caused a low penetrance of fusion specifically between the third and fourth sternebrae (13/43, Fig. 3F), as previously described (Green, 1951). Homozygosity for the *bp* mutation affected the formation of particular sterno-costal joints (see Figs 3G, 4E; Table 3). 55 out of 58 *se/+; bp/bp* animals had ectopic mineralization in the rostral sterno-costal junctions, suggesting incomplete formation of the normal fibrocartilage joint between these structures. This phenotype varied from small, independent ossified regions within the fibrocartilage, to larger extensions of bone continuous with the caudal end of the rostral sternebra (see Fig. 3G). This ectopic ossification was limited to the joints where rib pairs two and three articulate with the sternum (Table 3; Fig. 4E).

When both the *se* and the *bp* mutations were homozygous, ectopic mineralization was generally more severe and was observed in joints not affected in either single mutant. For example, at the joints where rib pair 4 and 5 articulate, there was ectopic mineralization in 75-100% of the double mutant sternums analyzed (see Table 3; Fig. 4E). These sites were largely unaffected in single mutants. In addition to ectopic mineralization, double mutant animals also showed frequent partial to complete fusion of the ribs with the sternum (Table 3; Fig. 3H-J). Interestingly, there was a strong correlation between the frequency of rib fusions and the presence of adjacent sternebrae. Rib separation was only affected in 13% of the ribs that articulated between two unaffected sternebrae. This percentage increased to 80% when there was a single missing adjacent sternebrae and to 100% when both adjacent sternebrae were missing (Table 3).

Sternum histology in double mutants

To investigate the origin of the sternum phenotypes, we examined embryos of wild-type and double mutant mice. Previous studies (Chen, 1952a,b) have shown that the sternum arises from two mesodermal condensations (sternal bands) that originate in the dorsal lateral wall of the embryo. These condensations elongate in the caudal direction while moving towards, and eventually meeting at, the ventral midline. Ribs arise independently of the sternal bands, grow towards the ventral midline and transiently fuse with the sternal bands to generate a single chondrifying unit. Most of the cartilage in the sternal bands continues to differentiate, hypertrophy and is eventually replaced by bone. At the sites where the ribs contact the sternum, however, hypertrophy and ossification are inhibited resulting in the formation of a compound fibrocartilaginous joint between the rib pair and the adjacent sternebrae. Addition and removal of ribs in organ culture has shown that segmentation and joint formation in the sternum is induced by a signal from the ribs (Chen, 1953).

Although, in adult double mutants, sternebrae were completely missing from the mid-sternum, in embryos, sternal bands were initially present and continuous rostrally and caudally (Fig. 5B and data not shown). At this stage, the only detectable difference between wild-type and double mutants is a delay in the arrival of the sternal bands at the ventral midline by approximately 0.5 days. Once at the midline, the sternal bands of wild-type embryos increase in thickness and continue to differentiate into cartilage (Fig. 5C). In the double mutants, although the most rostral and caudal regions of the sternum increase in width and continue to differentiate, in the region where rib pairs 3 and 4 are located, the sternal bands remain thin and relatively undifferentiated (Fig. 5D). The ribs in this region appear to continue to grow towards the ventral midline, ‘squeezing’ the thin sternal bands together and appearing to almost make contact with one another (see Fig. 5D). The sternal bands in this region never proliferate and eventually degenerate or become incorporated into the fused ribs. The remaining space where the sternebra should be is filled with muscle and connective tissue (Fig. 5F).

A second phenotype observed in the adult mutant sternums was the failure to form normal sterno-costal joints. In wild-type mice, the initial signs of segmentation are the organization of flattened cells around the rib tips, and the inhibition of both matrix production and cartilage hypertrophy in the regions were the ribs make contact. Both features are apparent by embryonic day 16. At a similar stage in the development of the double mutant, these cellular changes were not apparent. Matrix deposition was not inhibited and the rib tips were not as clearly demarcated (Fig. 5E,F).

The histological studies suggest that the initial sternal condensations and the rib/sternum complex form normally in *se/se; bp/bp* double mutant embryos. The adult phenotypes appear to arise from a failure of the sternal bands to increase in thickness in the midportion of the sternum. In other regions, sternal cartilage forms, but does not exhibit the regional differences in cartilage maturation and hypertrophy that are normally seen adjacent to ribs. These studies suggest that *Bmp5* and *Gdf5* are required for regional differentiation of the

sternal bands, and for the normal formation of the fibrocartilaginous joints at sterno-costal junctions.

Bmp5 and *Gdf5* expression during sternum development

To better understand the functions of *Bmp5* and *Gdf5* in sternum development, we analyzed the RNA expression pattern of both genes at three consecutive stages: prior to the fusion of the sternal bands and ribs at the midline, just after the ribs and sternal bands have reached the ventral midline, and once the sternal bands have increased in thickness (stages 2-4 in the staging system described by Chen). *Bmp5* is expressed in the perichondrium surrounding the ribs and the sternal bands at all stages examined, beginning before the fusion of the sternal bands (Fig. 6A) and continuing through the formation of the rib/sternum complex and the first signs of segmentation of the ribs and the sternebrae (see Fig. 6C,E and data not shown). *Bmp5* is also expressed throughout the condensation for the xiphoid process (data not shown).

The pattern of *Gdf5* expression was more dynamic. At early stages when *Bmp5* was clearly expressed in the perichondrium, *Gdf5* was expressed in a nearly complementary pattern in the procartilage of the separate sternal bands and ribs (Fig. 6B). At subsequent stages, once the rib/sternum complex has formed at the midline, *Gdf5* expression became restricted to small stripes localized to the rib/sternum junctions (see Fig. 6D,F). This expression was observed at the junctions of rib pairs 2-7; but not the junction of rib pair 1 (Fig. 6D and data not shown). *Gdf5* expression was maintained at the sterno-costal junctions at least through stage 5 of sternum development, when the segmental hypertrophy of the sternebrae becomes apparent. Thus, the late pattern of *Gdf5* expression in the sternum was restricted to the regions of joint formation, suggesting that, analogous to its role in limb development, *Gdf5* may also have a function in joint development in the sternum.

DISCUSSION

Initial studies of *Gdf5* reported that the gene was expressed in and around skeletal precursors and, in the developing limbs but not in axial skeletal structures (Chang et al., 1994; Storm et al., 1994). The more detailed studies reported here show that *Gdf5* is expressed in a series of stripes in the developing limbs and sternal elements, and that the position, number and order of appearance of these stripes corresponds to the position, number and order of appearance of the joints that form within these structures.

Despite the importance of joint formation in skeletal patterning and human disease, relatively little is known about the molecular mechanisms that control where and when a joint will form. In the limb, joints typically arise by the splitting of larger skeletal precursors, rather than by the collision or apposition of separate elements. This process takes place through a series of steps including (1) initial formation of specialized regions of high cell density (interzones) that extend in transverse stripes across developing cartilage elements, (2) programmed cell death and changes in matrix production in the center of the interzone, creating a three-layered structure, (3) differentiation of articular cartilage at the two edges of the interzone and (4) accumulation of fluid-filled spaces that coalesce to make a gap between opposing skeletal elements (cavitation) (Haines, 1947; Mitrovic, 1978; Craig et al., 1987; Little and Mirkes, 1995; Nalin et al., 1995), Ligaments, synovial membranes and tendon insertions develop from additional lateral condensations surrounding the developing joint. In rodents, the time between interzone formation and completion of cavitation is usually 4 days or more (Mitrovic, 1978). Formation and maintenance of the joint cavity is dependent on muscular activity, but the initial positioning and cellular changes during joint development appear to be specified independently of either muscle activity or growth of adjacent elements (Fell and Canti, 1934; Drachman and Sokoloff, 1966; Holder, 1977).

Gdf5 represents one of the only known molecular markers for the early stages of joint formation. Expression is initiated in the region of joint development 24 to 36 hours before the morphological appearance of the interzone (Dalgleish, 1964; Mitrovic, 1978). The expression continues for at least 2-3 days at a particular site, and is still evident at the three-layered interzone stage of joint development (for example, in the shoulder and elbow at 13.5 dpc, and in the digits at 14.5 dpc). Expression becomes increasingly difficult to detect at later stages of joint differentiation. This may in part be due to technical limitations of the in situ hybridization technique and the adult expression pattern of *Gdf5* remains to be investigated.

Null mutations in *Gdf5* provide a crucial test of the functional importance of this gene in the formation of synovial joints. Frameshift mutations at the mouse *brachypodism* locus disrupt the formation of approximately 30% of the joints in the limbs. This includes the complete absence of joint development between the proximal and medial phalanges in the forefeet and hindfeet, fusions of sesamoid bones in the digits, fusion of bones in the wrists and ankles, and abnormal development of joint structures in the knee. Although not yet as extensively studied, loss-of-function mutations at the human *Gdf5* locus also lead to defective formation of many joints, including loss of bones in the digits and dislocations of the hips and knees (Langer et al., 1989; Thomas et al., 1996).

How does disruption of *Gdf5* function lead to alterations in joint structures? Previous developmental, histological and histochemical studies of digit development in *brachypodism* mice suggest that mutations in *Gdf5* disrupt the initial cleavage of digital rays into the separate elements (Milaire, 1965; Grüneberg and Lee, 1973). The size and shape of the early limb bud is normal in *brachypodism* mice and the initial digital ray condensations are as long as in wild type, although somewhat thinner. Major differences in development are first observed between embryonic days 12.5 and 14.5, when the digital ray is beginning to segment. In *brachypodism* mice, the central part of the digital ray fails to develop an interzone and there is a subsequent failure to separate the proximal and medial phalanges. This produces a single combined element in the mutant digits, whose initial length is equal to or exceeds the combined length of the proximal and medial phalanges that form in wild-type digits (Grüneberg and Lee, 1973). This early segmentation defect is observed at a site where *Gdf5* is highly expressed, strongly suggesting that the *Gdf5* gene product plays a direct role in this segmentation process. In an excellent review of the classical embryological and histochemical studies on *brachypodism* mice, Hinchliffe and Johnson (1980) speculated that mutations at the *brachypodism* locus cause ‘a disruption in the usual pattern determining where joints are to

occur in the limb.' This hypothesis is strongly supported by the striking expression pattern of the *Gdf5* gene.

Although *Gdf5 is* expressed in nearly all the synovial joints of the limb, only a subset of the joints are disrupted by *brachypodism* null mutations. We think it is likely that other members of the BMP family may provide partially overlapping functions that compensate for loss of *Gdf5* at some locations. The mature signaling region of the GDF5 protein shares 80-90% amino acid sequence identity with GDF6 and GDF7, and approximately 50-60% identity with BMPs 2,4,5,6,7 and 8 (Storm et al., 1994). The closely related *Gdf6* and *Gdf7* genes are also expressed in and around developing joints (Hattersley et al., 1995; Wolfman et al., 1995; Storm, Settle and Kingsley, unpublished data) and are the most obvious candidates for overlapping functions. We are currently inactivating both *Gdf6* and *Gdf7* in order to test their individual functions in joint development, and their functional overlap with *Gdf5*.

Null mutations in the BMP family member, *Bmp5*, are already available from extensive genetic studies of the *short ear* locus (Kingsley et al., 1992; King et al., 1994). The phenotypes of mice missing both *Gdf5* and *Bmp5* have identified additional sites of action of *Gdf5* during embryonic development. Double mutant animals show a greater range of skeletal defects than those predicted from the individual phenotypes of *brachypodism* or *short ear* mice, including novel defects in the formation and segmentation of the sternum. Both *Bmp5* and *Gdf5* are clearly expressed in developing sternal structures, but in largely non-overlapping patterns. The synergistic effect of the mutations may thus be due to eliminating the function of genes in parallel cellular pathways that contribute to the growth and segmentation of the sternum. For example, the growth in width of sternal bands may normally be influenced both by early expression of *Gdf5* within the sternal bands (Fig. 6B), and by expression of *Bmp5* in the perichondrium surrounding the sternum (Fig. 6A,C,E). Inactivation of both *Bmp5* and *Gdf5* would disrupt both pathways, leading to a synergistic effect on sternebrae development. Similar effects may account for the effects of *Bmp5* and *Gdf5* mutations on limb elements, where the two genes are again expressed in largely nonoverlapping patterns in either perichondrium (King et al., 1994) or interzones (this paper).

The development and segmentation of the sternum provides an interesting contrast to the development of articulated skeletal structures in other regions of the body. Ribs and sternal bands originally arise as separate skeletal precursors, fuse transiently at the ventral midline and, subsequently, form a series of repeating sternebrae separated by joints at the sites of rib/sternal contact (Chen, 1952a,b, 1953). This segmentation takes place at a much later stage of cartilage differentiation than is seen in limbs, and the individual sternebrae and ribs remain connected by fibrocartilage rather than by true synovial joints. Despite the apparent differences between joint formation in the limb and the sternum, *Gdf5* is expressed in a stripe-like pattern at the sites of segmentation events in both structures. At the one rib/sternal contact site where segmentation does not occur in mice and most other mammals (the contact between the first rib and the manubrium, Parker, 1867), *Gdf5* expression is not detected, further strengthening the association between *Gdf5* expression and segmentation events in sternal development. The expression of *Gdf5* in regions of joint development in both limb elements and the sternum, and the defects in joint formation at both sites in mutant animals, suggest that *Gdf5* plays an important role in formation of both diarthrodial (synovial) and synchondrial (fibrocartilaginous) joints. Several other specialized types of joints are known (Gray, 1901) and it will be interesting to test whether *Gdf5* functions in the development of other contacts between skeletal structures.

Although alteration in the number and connection of skeletal elements is one of the most obvious changes in *brachypodism* mice, *Gdf5* mutations also alter the number and insertions of various tendons in the limbs, and the length of many of the long bones (Grüneberg and Lee, 1973, this paper). Most tendons insert in and around joints, and the expression of *Gdf5* in joints and along the edges of several skeletal elements, could directly or indirectly influence tendon formation. Interestingly, preliminary reports suggest that proteins closely related to *Gdf5* may be capable of inducing the formation of connective tissue resembling tendons and ligaments when implanted subcutaneously in adult animals (Wolfman et al., 1995). Reduction in the length of the long bones appears to be the result of several factors. Most of the longitudinal growth of skeletal elements depends upon division and hypertrophy of cartilage cells at the ends of the elements. The altered pattern of segmentation in *brachypodism* digital rays reduces the number of ends where growth can occur, by reducing the overall number of elements in the limb. With fewer ends, there are fewer regions that contribute to longitudinal growth. In addition, growth plates are missing from the ends of metacarpals and metatarsals (Table 1), and there is a reduced height and mitotic rate in the growth plates in other skeletal elements after birth (Nakamura et al., 1984). Expression of *Gdf5* may thus affect not only the position and number of early segmentation events, but also the subsequent growth of the resulting elements.

Comparative studies of limb development in amphibians, urodoles, reptiles, birds and mammals suggest that the overall pattern of skeletal structures emerges from a combination of three fundamental morphogenetic behaviors of mesenchyme: the aggregation of cells into precursors of future skeletal elements, the branching of many of these precursors and the segmentation or splitting of condensations into separate daughter elements connected by joints (Shubin and Alberch, 1986; Oster et al., 1988). Members of the BMP family have previously been implicated in the de novo formation of skeletal condensations (Kingsley, 1994b for review). The current studies suggest that other members of the BMP family may also play essential roles in the segmentation process that generates the joints between the skeletal elements. This function must require a distinct set of cellular responses within a skeletal condensation, presumably including changes in both cell adhesion and programmed cell death. A large body of previous work has shown that various BMP family members can induce many different responses in developing tissues (Kingsley, 1994a; Hogan, 1996), including stimulation of programmed cell death in both rhombomeres (Graham et al., 1994) and limb bud interdigit mesenchyme (Zou and Niswander, 1996). Further study of the regulation and cellular responses to *Gdf5* may help identify many of the molecular events that control the formation of joints in the vertebrate skeleton.

We would like to thank Maylene Wagener for excellent animal

care, and Ralph DiLeone, Jennifer King, Greg Marcus and Michael Schoor for helpful comments on the manuscript. This work was supported in part by grants from the National Institutes of Health and the Lucille P. Markey Charitable Trust (D. M. K.) and by a Lieberman Graduate Fellowship (E. S.). D. M. K. is a Lucille P. Markey Scholar in Biomedical Science.

REFERENCES

Chang, S. C., Hoang, B., Thomas, J. T., Vukicevic, S., Luyten, F. P., Ryba, N. J., Kozak, C. A., Reddi, A. H. and Moos Jr., M. (1994). Cartilage-derived morphogenetic proteins. New members of the transforming growth factor-beta superfamily predominantly expressed in long bones during human embryonic development. *J. Biol.C hem.* **269**, 28227-34.

Chen, J. M. (1952a). Studies on the morphogenesis of the mouse sternum. I. Normal embryonic development. *J. Anat., Lond.* **86**, 373-386.

Chen, J. M. (1952b). Studies on the morphogenesis of the mouse sternum. II Experiments on the origin of the sternum and its capacity for self-differentiation in vitro. *J. Anat., Lond.* **86**, 387-401.

Chen, J. M. (1953). Studies on the morphogenesis of the mouse sternum. III. Experiments on the closure and segmentation of sternal bands. *J. Anat., Lond.* **87**, 132-149.

Craig, F. M., Bentley, G. and Archer, C. W. (1987). The spatial and temporal pattern of collagens I and II and keratan sulphate in the developing chick metatarsophalangeal joint. *Development* **99**, 383-91.

Dalgleish, A. E. (1964). *Development of the Limbs of the Mouse*. Stanford University Ph.D. Thesis.

Drachman, D. B. and Sokoloff, L. (1966). The role of movement in embryonic joint development. *Dev. Biol.* **14**, 401-420.

Elmer, W. A. and Selleck, D. K. (1975). In vitro chondrogenesis of limb mesoderm from normal and brachypod mouse embryos. *J. Embryol. Exp. Morph.* **33**, 371-386.

Fell, H. B. and Canti, R. G. (1934). Experiments on the development in vitro of the avian knee-joint. *Proc. Royal Soc. B* **116**, 316-327.

Graham, A., Francis, W. P., Brickell, P. and Lumsden, A. (1994). The signalling molecule BMP4 mediates apoptosis in the rhombencephalic neural crest. *Nature* **372**, 684-6.

Gray, H. (1901). *Anatomy, Descriptive and Surgical*. Philadelphia: Running Press.

Green, M. C. (1951). Further morphological effects of the short ear gene in the house mouse. *J. Morphol.* **88**, 1-22.

Green, M. C. (1968). Mechanism of the pleiotropic effects of the short ear mutant gene in the mouse. *J. Exp. Zool.* **167**, 129-150.

Grüneberg, H. and Lee, A. J. (1973). The anatomy and development of brachypodism in the mouse. *J. Embryol. Exp. Morph.* **30**, 119-141.

Haines, R. W. (1947). The development of joints. *J. Anat.* **81**, 3-55.

Hall, B. K. and Miyake, T. (1992). The membranous skeleton: the role of cell condensations in vertebrate skeletogenesis. *Anat. Embryol.* **186**, 107-124.

Hattersley, G., Hewick, R. and Rosen, V. (1995). In situ localization and in vitro activity of BMP-13. *J. Bone Min. Res.* **10**, S163.

Hinchliffe, J. R. and Johnson, D. R. (1980). *The Development of the Vertebrate Limb*. Oxford: Clarendon Press.

Hogan, B. L. M. (1996). Bone morphogenetic proteins: multifunctional regulators of vertebrate development. *Genes Dev.* **10**, 1580-1594.

Holder, N. (1977). An experimental investigation into the early development of the chick elbow joint. *J. Embryol. Exp. Morph.* **39**, 115-127.

King, J. A., Marker, P. C., Seung, K. J. and Kingsley, D. M. (1994). BMP5 and the molecular, skeletal, and soft-tissue alterations in short ear mice. *Dev. Biol.* **166**, 112-122.

King, J. A., Storm, E. E., Marker, P. C., DiLeone, R. and Kingsley, D. M. (1996). The role of BMPs and GDFs in development of region-specific skeletal structures. *Annals New York Acad. Sci. USA* **785**, 70-79.

Kingsley, D. M. (1994a). The TGF-beta superfamily: new members, new receptors, and new genetic tests of function in different organisms. *Genes Dev.* **8**, 133-146.

Kingsley, D. M. (1994b). What do BMPs do in mammals? Clues from the mouse short ear mutation. *Trends Genet.* **10**, 16-21.

Kingsley, D. M., Bland, A. E., Grubber, J. M., Marker, P. C., Russell, L. B., Copeland, N. G. and Jenkins, N. A. (1992). The mouse *short ear* skeletal morphogenesis locus is associated with defects in a bone morphogenetic member of the TGF-β superfamily. *Cell* **71**, 399-410.

Landauer, W. (1952). Brachypodism, a recessive mutation of house mice. *J. Heredity* **43**, 293-298.

Langer, L. J., Cervenka, J. and Camargo, M. (1989). A severe autosomal recessive acromesomelic dysplasia, the Hunter-Thompson type, and comparison with the Grebe type. *Hum. Genet.* **81**, 323-8.

Little, S. A. and Mirkes, P. E. (1995). Clusterin expression during programmed and teratogen-induced cell death in the postimplantation rat embryo. *Teratology* **52**, 41-54.

Lufkin, T., Mark, M., Hart, C. P., Dolle, P., LeMeur, M. and Chambon, P. (1992). Homeotic transformation of the occipital bones of the skull by ectopic expression of a homeobox gene. *Nature* **359**, 835-41.

Lyons, K. M., Pelton, R. W. and Hogan, B. L. (1989). Patterns of expression of murine Vgr-1 and BMP-2a RNA suggest that transforming growth factor-beta-like genes coordinately regulate aspects of embryonic development. *Genes Dev.* **3**, 1657-1668.

Mikic, B., van der Meulen, M. C. H., Kingsley, D. M. and Carter, D. R. (1995). Long bone geometry and strength in adult BMP-5 deficient mice. *Bone* **16**, 445-454.

Mikic, B., van der Meulen, M. C. H., Kingsley, D. M. and Carter, D. R. (1996). Mechanical and geometric changes in the growing femora of BMP-5 deficient mice. *Bone* (in press).

Milaire, J. (1965). Étude morphogénétique de trois malformations congénitales de l'autopode chez la souris (syndactylisme – brachypodisme – Hémimélie dominante) par des méthodes cytochimiques. *Académie Royale de Belgique, Classe de Science. Mémoires* **16**, 1-120.

Mitrovic, D. (1978). Development of the diarthrodial joints in the rat embryo. *Am. J. Anat.* **151**, 475-85.

Nakamura, K., Hirosawa, K., Hama, K. and Oda, S. (1984). Defects in the growth plate of brachypodism in mice--light and electron microscopic findings and cell proliferation by the method of tritiated thymidine autoradiography. *Nippon Seikeigeka Gakkai Zasshi* **58**, 835-45.

Nalin, A. M., Greenlee, T. K. J. and Sandell, L. J. (1995). Collagen gene expression during development of avian synovial joints: transient expression of types II and XI collagen genes in the joint capsule. *Dev. Dynamics* **203**, 352-362.

Oster, G. F., Shubin, N., Murray, J. D. and Alberch, P. (1988). Evolution and morphogenetic rules: the shape of the vertebrate limb in ontogeny and phylogeny. *Evolution* **42**, 862-884.

Parker, W. K. (1867). *On the Structure and Development of the Shoulder-girdle and Sternum in the Vertebrata*. Piccadilly: Robert Hardwicke.

Reddi, A. H. and Huggins, C. (1972). Biochemical sequences in the transformation of normal fibroblasts in adolescent rats. *Proc. Natl. Acad. Sci. USA* **69**, 1601-1605.

Rosen, V. and Thies, R. S. (1992). The BMP proteins in bone formation and repair. *Trends Genet* **8**, 97-102.

Schaeren-Wiemers, N. and Gerfin-Moser, A. (1993). A single protocol to detect transcripts of various types and expression levels in neural tissue and cultured cells: in situ hybridization using digoxigenin-labelled cRNA probes. *Histochemistry* **100**, 431-40.

Shubin, N. H. and Alberch, P. (1986). A morphogenetic approach to the origin and basic organization of the tetrapod limb. *Evolutionary Biol.* **20**, 319-387.

Storm, E. E., Huynh, T. V., Copeland, N. G., Jenkins, N. A., Kingsley, D. M. and Lee, S.-L. (1994). Limb alterations in brachypodism mice due to mutations in a new member of the TGF-beta superfamily. *Nature* **368**, 639-643.

Thomas, J. T., Lin, K., Nandedkar, M., Camargo, M., Cervenka, J. and Luyten, F. P. (1996). A human chondrodysplasia due to a mutation in a TGF-B superfamily member. *Nature Genet.* **12**,

Urist, M. R. (1965). Bone. Formation by autoinduction. *Science* **150**, 893-899.

Wanek, N., Muneoka, K., Holler, D. G., Burton, R. and Bryant, S. V. (1989). A staging system for mouse limb development. *J. Exp. Zool.* **249**, 41-9.

Wolfman, N. M., Celeste, A. J., Cox, K., Hattersley, G., Nelson, R., Yamaji, N., DiBlasio-Smith, E., Nova, J., Song, J. J., Wozney, J. M. and Rosen, V. (1995). Preliminary characterization of the biological activities of rhBMP-12. *J. Bone Min. Res.* **10**, S148.

Zou, H. and Niswander, L. (1996). Requirement for BMP signaling in interdigital apoptosis and scale formation. *Science* **272**, 738-741.

(Accepted 4 September 1996)